Microstructure within domains of melt-processed $YBa_2Cu_3O_{7-x}$ superconductors

K. B. Alexander, A. Goyal, and D. M. Kroeger
Oak Ridge National Laboratory, P.O. Box 2008, Oak Ridge, Tennessee 37831-6068

V. Selvamanickam and K. Salama
Oak Ridge National Laboratory, P.O. Box 2008, Oak Ridge, Tennessee 37831-6068
and Texas Center for Superconductivity at University of Houston, Houston, Texas 77004
(Received 30 September 1991)

The microstructure within single domains of melt-processed $YBa_2Cu_3O_{7-x}$ (1:2:3) material has been examined. Rather than composing a "brick-wall" structure, the stacked, parallel platelets within the domains are actually portions of a single crystal. A growth mechanism is proposed that is consistent with the observed microstructural features. The anisotropic nature of the growth of 1:2:3 results in gaps separating the platelets. The gaps, however, terminate within domains, resulting in interconnected single-crystalline material. The absence of weak-link behavior for current flow along the *c* axis and the high critical-current densities observed within domains of melt-processed 1:2:3 material are readily explained by the fact that current flow is solely through single-crystalline material.

INTRODUCTION

The attainment of high critical-current densities in high-temperature superconductors has been an important goal since the discovery of these materials.[1] Although high critical currents in excess of 10^5 A/cm^2 at 77 K and 1 T have been achieved in epitaxial thin films of 1:2:3,[2] polycrystalline, bulk sintered materials typically have critical-current densities several orders of magnitude lower which furthermore decrease rapidly in the presence of applied magnetic fields. The lower critical-current densities of bulk 1:2:3 material have been attributed primarily to poor current transmission at grain boundaries, with the intrinsic anisotropy of J_c playing a minor role. The role of grain boundaries in 1:2:3 materials has been demonstrated by Chaudhari *et al.* and Dimos *et al.* in studies of the critical current density across individual grain boundaries.[3,4] In general, grain boundaries have been shown to act as Josephson junctions, and thus as weak links to current flow.[3,5,6] Recent work by Babcock *et al.* on individual bulk grain boundaries, however, has shown that not all grain boundaries necessarily act as weak links.[7]

Efforts have been made to improve the critical-current density of bulk materials by grain alignment to produce highly textured microstructures. Melt-textured materials are known to exhibit critical-current densities in excess of 10^4 A/cm^2 at 77 K.[8–11] Salama *et al.* reported a critical-current density in excess of 3.7×10^4 A/cm^2 in a 0.6-T field at 77 K for single domains cut from 1:2:3 melt-processed material.[12] The domains consisted of many stacked platelets having a common *c* axis. This stacked-platelet microstructure has been described as a "brick-wall" microstructure.[13,14] In a brick-wall structure, the platelets possess a common, or nearly common *c* axis; rotations about this *c* axis result in twist boundaries (with a small or negligible tilt component) between stacked platelets.[13,14] High-angle boundaries are presumed to exist between adjacent platelets within the *a*-*b* plane in a brick-wall microstructure. Recently, however, resistive measurements of J_c in single-domain specimens cut with their *c* axes at various angles to the specimen axis demonstrated that current transmission in the *c* direction was not weak-link limited.[15] Although the critical-current density decreased with an increase in the number of platelets crossed (as determined by the direction of the *c* axis relative to the specimen axis), J_c remained relatively insensitive to magnetic field, indicating that the boundaries between platelets were not weak links. It was suggested that the boundaries within the melt-textured domains are different in character than those in bulk sintered 1:2:3 materials.[15] The purpose of this work is to examine the boundaries between the platelets within single domains to determine their crystallography and chemistry and to relate these observations to the reported superconducting behavior of these materials.

EXPERIMENTAL PROCEDURE

Highly aligned 1:2:3 was prepared by rapidly heating sintered material into the liquid and 2:1:1 region of the phase diagram. The specimens were then slowly cooled at a rate of 1–2 °C/h through the peritectic temperature.[12,15–17] After cooling to room temperature, the materials were annealed in oxygen at intermediate temperatures, 400–600 °C, for several hours. The specimens typically consist of large domains, each up to 6–10 mm long, depending on the exact processing conditions.

Specimens were prepared from isolated single domains for transmission electron microscopy (TEM) examination by mechanical thinning followed by ion milling with a liquid-nitrogen-cooled stage. All TEM studies were performed with the use of a liquid-nitrogen-cooled specimen holder.

RESULTS AND DISCUSSION

It should be emphasized that the observations discussed herein only pertain to microstructural features within single domains of Y-Ba-Cu-O melt-processed (or melt-textured) materials. The domain microstructure consists of parallel stacked platelets of Y-Ba-Cu-O and

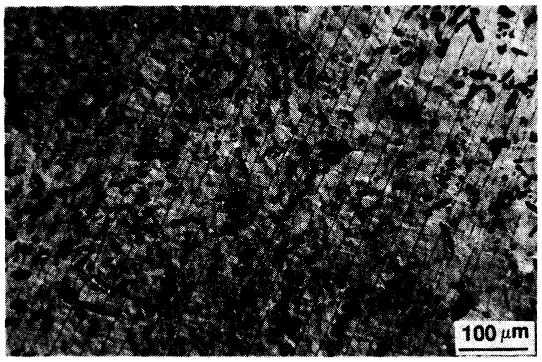

FIG. 1. Optical micrograph showing the structure within a domain of melt-processed Y-Ba-Cu-O material.

dispersed 2:1:1 phase, as shown in Fig. 1. Typically, 1:2:3 domains are identified by optical metallographic techniques. More detailed studies by the present authors using Nomarski interference imaging techniques often showed the presence of small-angle grain boundaries, which were not in general parallel to the basal plane, within metallographically defined domains. The effects of these small-angle boundaries on the properties of 1:2:3 materials are planned to be discussed in another paper.

Examination of the region between parallel platelets by TEM shows that the platelets are physically separated, as shown in Fig. 2. The gap region between the platelets is filled with material consisting primarily of copper oxides with some barium-copper oxides as well as some yttrium-rich material, as shown in Fig. 3. A region where the gap is completely filled with only crystalline copper and barium-copper oxides is shown in Fig. 4. Often, impurity elements such as Si, Mo, and S were also observed within the gap material.

Although cracks will form on cooling due to the thermal anisotropy of the 1:2:3 phase, the filled-in gaps cannot be explained solely on this basis. Any cracks that do form would contain either no material at all, or amorphous material resputtered during the ion-milling process. Since all ion-milling procedures were performed with liquid-nitrogen cooling, any resputtered material should not be able to crystallize. The oxygenation treatment after melt processing may affect the constituents present within the gap since decomposition of the 1:2:3 material may occur under these conditions.[18] In this case, the free surfaces formed by the cracks might decompose, but the decomposition products would not completely fill the gap. The microstructure shown in Fig. 4 is therefore inconsistent with these gaps resulting from the presence of cracks alone.

The platelets always terminate with an a-b plane parallel to the gap—that is, all the platelets within a domain had broad faces perpendicular to a common c axis. It has generally been assumed that the microstructure of these materials is a brick-wall structure and that these boundaries which are perpendicular to the c axis are simple twist boundaries.[13,14] Convergent beam electron diffraction (CBED), however, shows that there is virtually no orientation change between adjacent platelets, as shown in Fig. 5. All CBED patterns were obtained from either side of a gap region with a fine (<2 nm) probe placed as close to the gap region as possible. The largest measured misorientation change was 1.2°, which is within the realm of misorientation changes that would be induced by local specimen bending. Examination of many adjacent, as well as well-separated (up to 1 mm), platelets indicates that the platelets are actually portions of a common single crystal. Single domains of melt-processed materials from several sources[12,15–17] and processes have been examined and, in each case, the platelet crystallography was consistent with having arisen from a single-crystalline origin. Some other relevant observations can be obtained by detailed examination of the liquid-solid interface. The optical micrograph in Fig. 6(a) shows the growth fronts of two impinging domains in an incompletely processed specimen. The gaps between the plate-

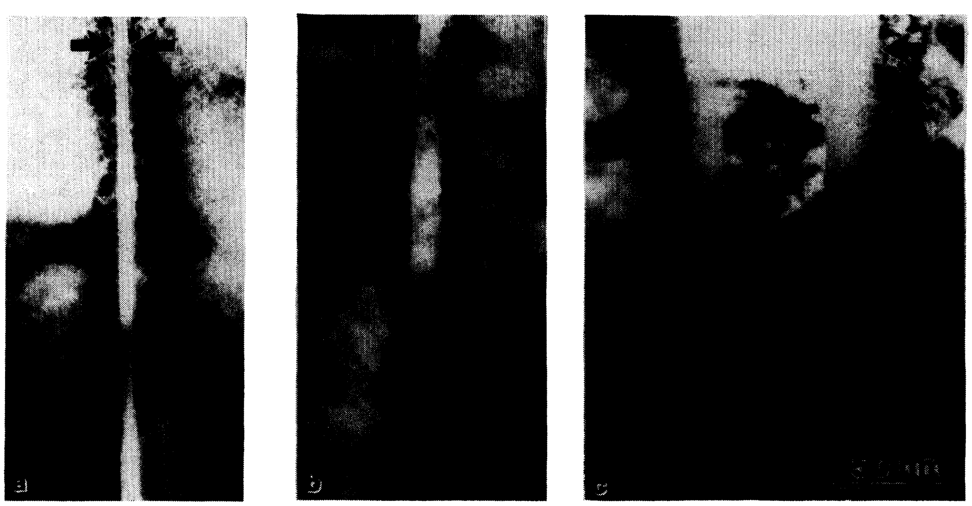

FIG. 2. (a)–(c) Typical TEM micrographs of the gap regions separating the parallel platelets within a domain of melt-processed Y-Ba-Cu-O.

lets often terminate (A) within a domain and the retained liquid phase often penetrates these gaps (B). These terminations are frequently observed on fracture surfaces, as demonstrated in the scanning electron microscopy (SEM) micrograph in Fig. 6(b). These gap terminations, along with the crystallographic evidence, suggest that the platelets are actually perfectly interconnected at, and beyond, these termination points.

Two platelets and the gap separating them are shown in Fig. 7(a). The gap between these platelets can be seen to terminate at the position marked "T." A higher magnification view of the termination is shown in Fig. 7(b), along with a portion of the gap as it narrows [Fig. 7(c)]. Beyond the gap termination, the lattice fringes (1.18 nm apart) associated with the *a*-*b* planes are continuous, and selected area and convergent beam electron diffraction shows that the material is crystallographically a single crystal. A gap termination in the proximity of a 2:1:1 particle is shown in Fig. 8.

The above observations suggest that a domain grows as a single crystal and that the gaps result from incomplete closure of the structure and are thus filled with rejected liquid phase during growth. The platelets grow primarily

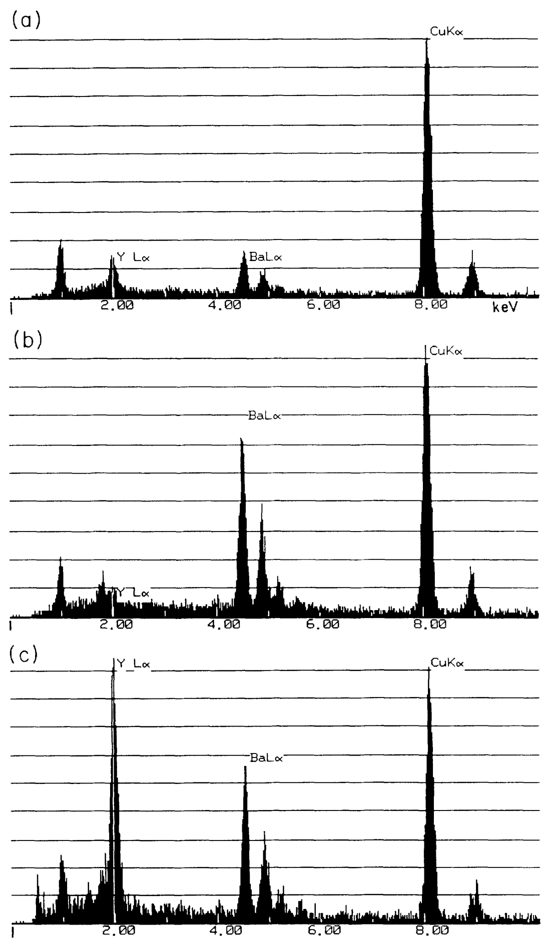

FIG. 3. Typical energy dispersive spectroscopy results from crystalline (a) and (b) and noncrystalline (c) phases within the gaps shown in Fig. 2.

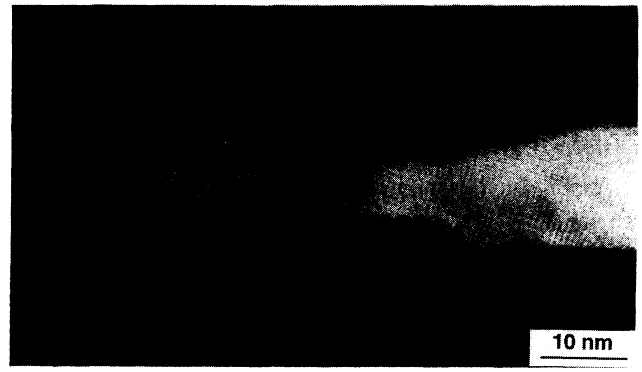

FIG. 4. Gap region that is filled only with crystalline copper oxide.

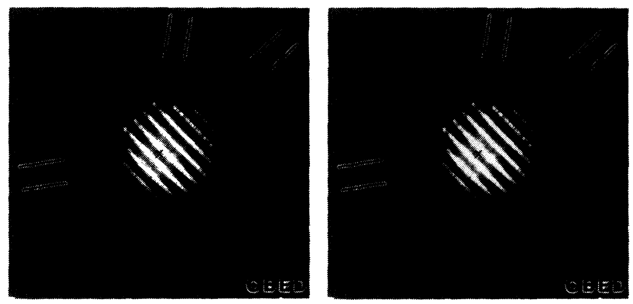

FIG. 5. Convergent beam electron diffraction patterns obtained from either side of a gap region.

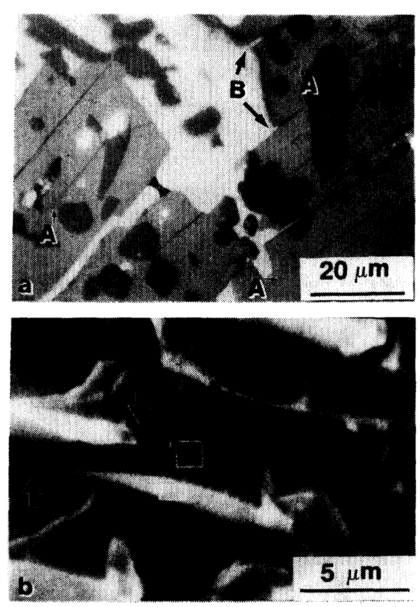

FIG. 6. (a) Optical micrograph of a growth front between several domains in melt-processed Y-Ba-Cu-O. Regions marked "A" show platelet terminations; regions marked "B" show the retained liquid phase penetrating the region between adjacent platelets. (b) SEM image of a fractured Y-Ba-Cu-O melt-processed domain showing terminations within the domain.

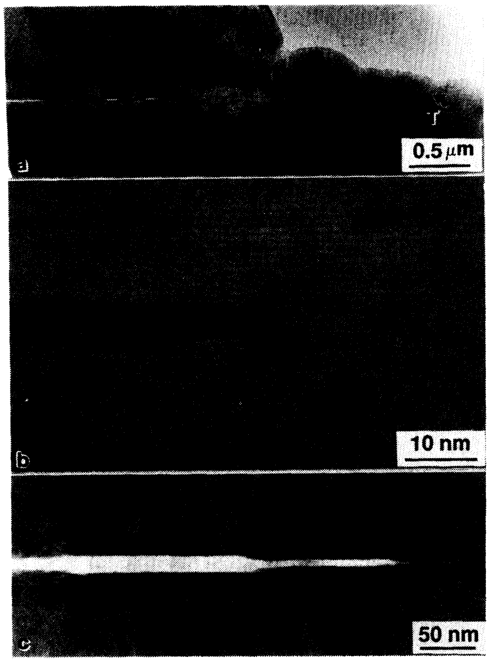

FIG. 7. (a) TEM image showing a gap terminating at the position marked "T." (b) Higher magnification image of the termination point showing that the material beyond the termination is continuous. (c) Region along the gap showing a stepwise narrowing of the gap.

by rapid, lateral ledge growth in the a-b plane. Growth along the c axis, perpendicular to the platelet broad face, however, is relatively slow. Perturbations at the growth front may result in a relatively rapid platelet extension in the a-b plane away from the macroscopic growth front. Compositional perturbations at the growth front are likely since the material ahead of the growth front is inherently inhomogeneous due to the presence of dispersed 2:1:1 particles in the liquid copper- and -barium-rich oxide phase. The resultant microstructure can be considered to be a two-dimensional analog of a traditional cellular solidification process, as shown in Fig. 9. The

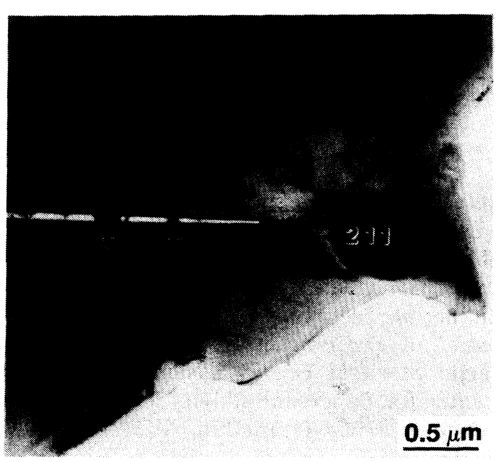

FIG. 8. Gap terminating near a 2:1:1 particle. The material to the right of the 2:1:1 particle is continuous. Diffraction contrast from crystalline material is seen within the gap region.

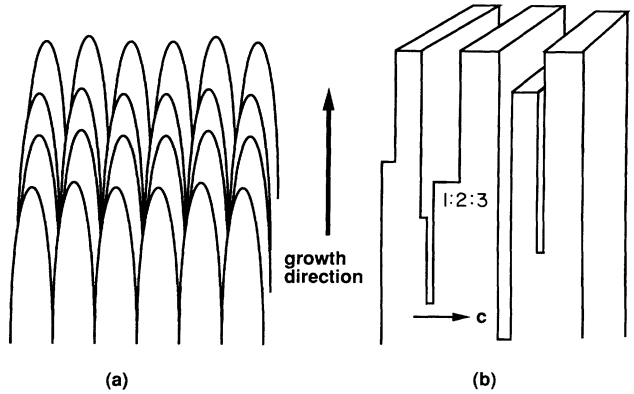

FIG. 9. (a) Typical growth front during cellular solidification. (b) Growth front during solidification of melt-processed Y-Ba-Cu-O material.

relatively slow growth normal to the platelet face, along with the long-range transport necessary along the gap, will ultimately limit the ability to heal the gaps completely.

The 2:1:1 particles may contribute to the gap-formation process. When the growth front abuts a 2:1:1 particle, nucleation on the 1:2:3 platelet broad face at the 2:1:1 interface is likely, as shown in Figs. 10(a) and 10(b). Once sufficient growth along the c direction occurs such that the 2:1:1 particle can be bypassed, rapid lateral growth occurs across the top of the 2:1:1 particle [Fig. 10(c)]. This may result in a gap on one side of the 2:1:1 particle if the 1:2:3 material did not envelop the 2:1:1 particle by growing at nearly identical rates on either side of the particle, as shown in Fig. 10(d).

Our observations are consistent with these proposed growth mechanisms. The resultant microstructure consists of platelets of identical orientation separated by gaps which are filled in with rejected liquid. The crystalline oxides (Fig. 3) and the impurity elements observed within

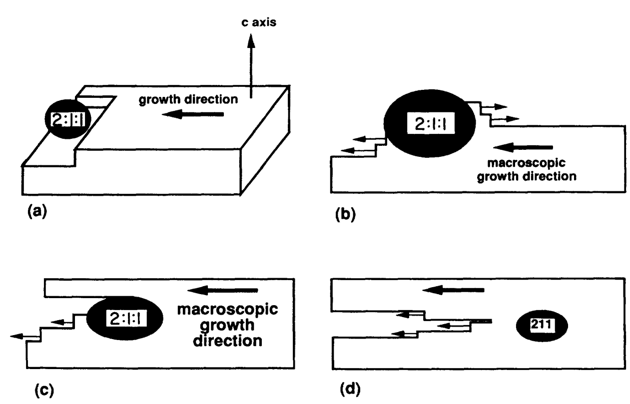

FIG. 10. Schematic of possible role of 2:1:1 particles on the growth of melt-processed Y-Ba-Cu-O. (a) Y-Ba-Cu-O platelet abuts a growing platelet. (b) Heterogeneous nucleation occurs at the platelet-2:1:1-liquid junction. (c) Once sufficient growth along the c direction occurs such that the 2:1:1 particle can be bypassed, rapid lateral growth will occur. (d) This process results in a gap, which may not heal completely.

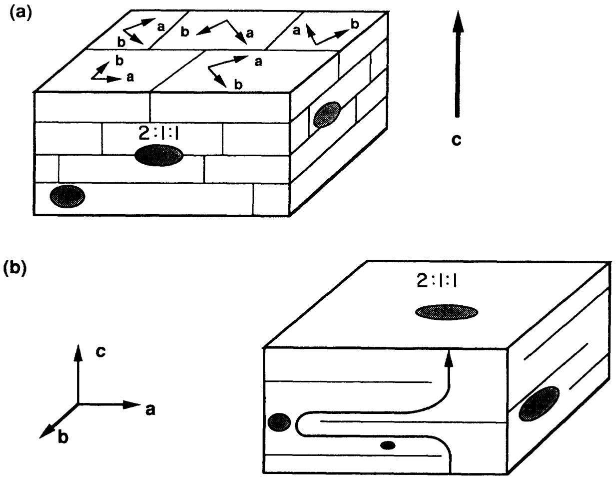

FIG. 11. (a) Schematic of a brick-wall microstructure. (b) Schematic proposed microstructure of 1:2:3 domains. Current flow along the *c* direction is solely through single-crystalline material within a domain of melt-processed Y-Ba-Cu-O.

the gap support this mechanism. The gap termination shown in Fig. 8 actually occurs near to a 2:1:1 particle, supplying further evidence for this model. The distribution of 2:1:1 particles has been suggested to be critical to the growth of high-quality melt-processed material. McGinn *et al.* have reported a decrease in platelet thickness with increasing amounts of 2:1:1,[19] whereas work by Jin *et al.*[20] showed that the platelet thickness scaled with the 2:1:1 particle size, and suggested that the 2:1:1 particles serve as nucleation sites for 1:2:3 growth as well as limit the platelet thickness. Recent work by the present authors on the melt processing of thick deposits of Y-Ba-Cu-O indicates that in spite of the presence of a high density of small 2:1:1 particles, typical isothermal melt-processing conditions result in the nucleation of relatively few 1:2:3 domains. Nevertheless, the presence of a high density of small 2:1:1 particles enhances the three-dimensional growth by increasing the growth rate in the *c* direction. Presumably, the three-dimensional growth is enhanced through a mechanism similar to that depicted in Fig. 10. Changing the processing conditions to increase the nucleation rate of 1:2:3 domains would result in a microstructure with many smaller, slightly misoriented domains (see, e.g., Ref. 21). The above model explains one possible role of 2:1:1 particles in the growth of these materials and appears to be consistent with the observed effects of 2:1:1 particles on the platelet thickness.[19,20]

Superconducting properties

The high critical-current densities and the non-weak-link behavior obtained in Y-Ba-Cu-O melt-processed materials can readily be explained by this model. A single domain of this material can be considered to be a single crystal. Unlike a brick-wall microstructure, which possesses high-angle grain boundaries perpendicular to the basal plane [Fig. 11(a)], there are no such boundaries in the present model [Fig. 11(b)] to impede current flow along the basal plane. The large critical-current densities observed for current flow in the basal plane in single-domain specimens are thus readily understood. For current flow along the *c* direction, a percolative path through continuous, interconnected single-crystalline regions can readily be envisioned in this material, as shown in Fig. 11(b). An increase in the number of interconnected regions would result in a larger effective cross section, and thus an increase in critical-current density for current flow along the *c* direction. This model thus also explains the observed absence of weak-link behavior for current flow in the *c* direction.

SUMMARY

The platelets within domains of Y-Ba-Cu-O melt-processed materials are simply portions of single crystal, not components of a brick-wall structure. These platelets are separated and the intervening region is often filled, primarily with crystalline copper and barium-copper oxides. A growth-mechanism model has been proposed to account for these observed microstructural features. The anisotropic nature of growth perpendicular (slow) and parallel (rapid) to the *a*-*b* plane results in "gaps" separating platelets. These gaps are filled with material consistent with the rejected liquid phase during 1:2:3 growth. These gaps terminate within the domains and, as a result, the platelets form an interconnected single crystal. The presence of 2:1:1 particles in the melt may be critical to enhancing growth along the *c* axis (Fig. 9) and thus to the formation of the large three-dimensional domains observed in melt-processed materials containing excess 2:1:1 particles.

The high critical-current densities and non-weak-link behavior of domains of melt-processed materials can be explained by current flow solely through single-crystalline Y-Ba-Cu-O material. Due to the presence of the nonsuperconducting gaps within the interconnected single-crystalline domains, the effective cross section for current flow is reduced. Therefore, in the absence of contributions from flux pinners in melt-processed Y-Ba-Cu-O,[22,23] the critical-current density, for current flow along the *c* direction, of these materials should be low relative to perfect single-crystalline Y-Ba-Cu-O.

ACKNOWLEDGMENTS

Our research has been sponsored by the U.S. Department of Energy, Assistant Secretary for Conservation and Renewable Energy, Office of Utility Technologies, Office of Energy Management/Advanced Utility Concepts-Superconducting Technology Program for Electric Energy Systems, under Contract No. DE-AC05-84OR21400 with Martin Marietta Energy Systems, Inc. and by the Texas Center for Superconductivity at the University of Houston under Prime Grant No. MDA 972-88-G-0002 from the Defense Advanced Research Projects Agency and the State of Texas.

[1]J. G. Bednorz and K. A. Mueller, Z. Phys. B **64**, 189 (1986).
[2]P. Chaudhari, R. H. Koch, R. B. Laibowitz, T. R. McGuire, and R. J. Gambuino, Phys. Rev. Lett. **51**, 852 (1987).
[3]P. Chaudhari, J. Mannhart, D. Dimos, C. C. Tsuei, J. Chi, M. M. Oprysko, and M. Scheuermann, Phys. Rev. Lett. **60**, 1653 (1988).
[4]D. Dimos, P. Chaudhari, J. Mannhart, and F. K. LeGoues, Phys. Rev. Lett. **61**, 219 (1988).
[5]D. P. Hampshire, X. Cai, J. Seuntjens, and D. C. Larbalestier, Supercond. Sci. Tech. **1**, 12 (1988).
[6]J. W. Ekin, A. I. Braginski, A. J. Panson, M. A. Janocko, D. W. Capone II, N. J. Zaluzec, B. Flandermeyer, F. O. F. deLima, M. Hong, J. Kwo, and S. H. Liou, J. Appl. Phys. **62**, 4821 (1987).
[7]S. E. Babcock, X. Y. Cai, L. Kaiser, and D. C. Larbalestier, Nature **347**, 167 (1990).
[8]S. Jin, T. H. Tiefel, R. C. Sherwood, M. E. Davis, R. B. van Dover, G. W. Kammlott, R. A. Fastnacht, and H. D. Keith, Appl. Phys. Lett. **52**, 2074 (1988).
[9]P. J. McGinn, W. Chen, N. Zhu, U. Balachandaran, and M. T. Lanagan, Physica C **165**, 480 (1990).
[10]M. Murakami, M. Morita, and N. Koyama, Jpn. J. Appl. Phys. **28**, L1125 (1989).
[11]R. L. Meng, C. Kinalidis, Y. Sun, L. Gao, Y. Tao, P. Hor, and C. W. Chu, Nature **345**, 326 (1990).
[12]K. Salama, V. Selvamanickam, L. Gao, and K. Sun, Appl. Phys. Lett. **54**, 2352 (1989).
[13]J. Mannhart and C. C. Tsuei, Z. Phys. B **77**, 53 (1989).
[14]A. P. Malozemoff, in *High-Temperature Superconducting Compounds II,* edited by S. H. Whang, A. DasGupta, and R. B. Laibowitz (TMS Publications, Warrendale, PA, 1990), p. 3.
[15]V. Selvamanickam and K. Salama, Appl. Phys. Lett. **57**, 1575 (1990).
[16]A. Goyal, P. D. Funkenbusch, D. M. Kroeger, and S. J. Burns, Physica C (to be published).
[17]G. Kozlowski, S. Rele, D. F. Lee, and K. Salama, J. Mater. Sci. **29**, 1056 (1991).
[18]R. K. Williams, K. B. Alexander, J. Brynestad, T. J. Henson, D. M. Kroeger, T. B. Lindemer, G. C. Marsh, and J. O. Scarborough, J. Appl. Phys. **67**, 6934 (1990).
[19]P. J. McGinn, W. Chen, N. Zhu, S. Sengupta, and T. Li, Physica C (to be published).
[20]S. Jin, G. W. Kammlott, T. H. Tiefel, T. T. Kodas, T. L. Ward, and D. M. Kroeger, Appl. Phys. Lett. (to be published).
[21]Y. Zhu, H. Zhang, H. Wang, and M. Suenaga, J. Mat. Res. (to be published).
[22]S. Jin, G. W. Kammlott, S. Nakahara, T. H. Tiefel, and J. E. Graebner, Science **253**, 42J (1991).
[23]M. Murakami, S. Gotoh, H. Fujimoto, K. Yamaguchi, N. Koshizuka, and S. Tanaka, Supercond. Sci. Tech. **4**, S43 (1991).

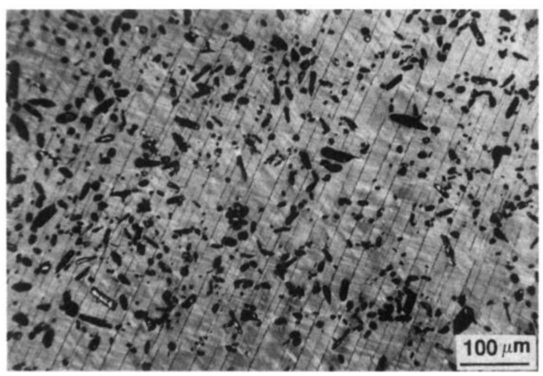

FIG. 1. Optical micrograph showing the structure within a domain of melt-processed Y-Ba-Cu-O material.

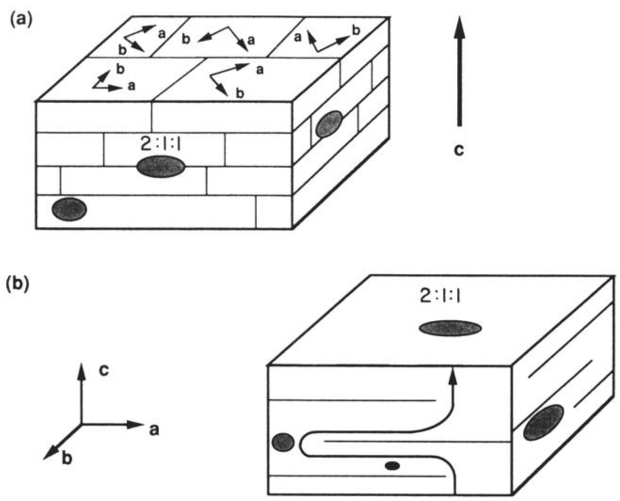

FIG. 11. (a) Schematic of a brick-wall microstructure. (b) Schematic proposed microstructure of 1:2:3 domains. Current flow along the c direction is solely through single-crystalline material within a domain of melt-processed Y-Ba-Cu-O.

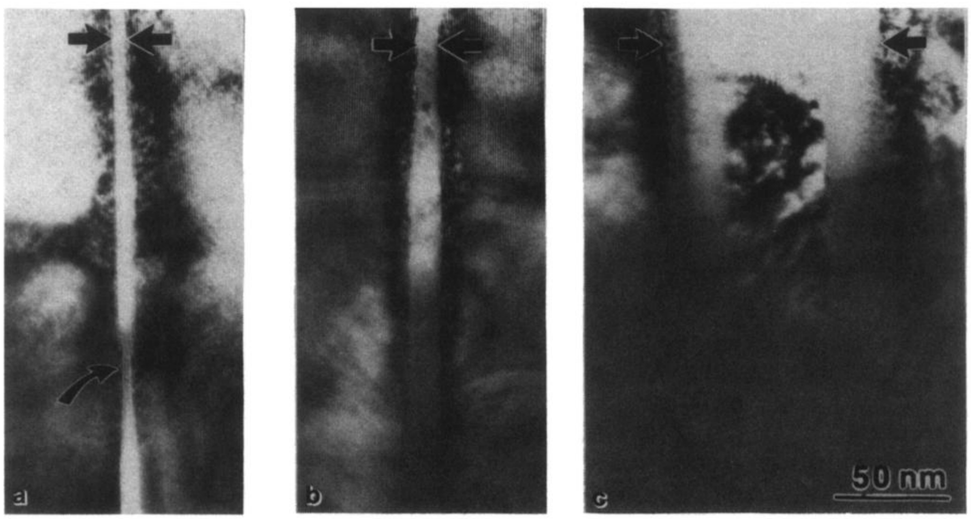

FIG. 2. (a)–(c) Typical TEM micrographs of the gap regions separating the parallel platelets within a domain of melt-processed Y-Ba-Cu-O.

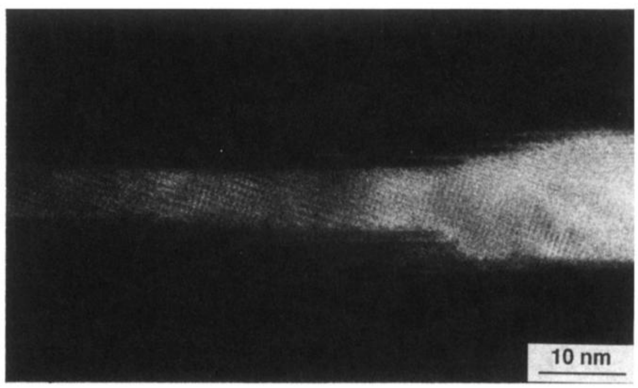

FIG. 4. Gap region that is filled only with crystalline copper oxide.

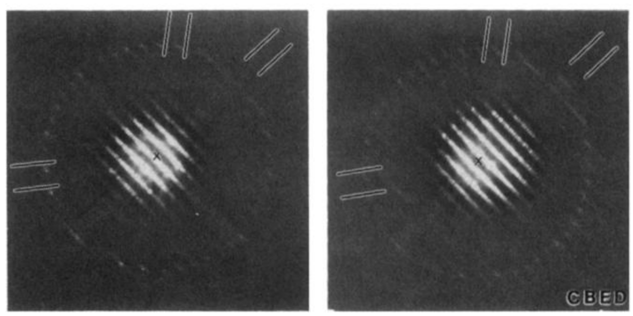

FIG. 5. Convergent beam electron diffraction patterns obtained from either side of a gap region.

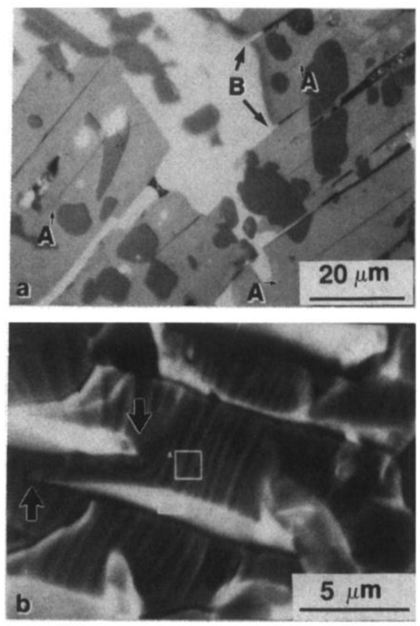

FIG. 6. (a) Optical micrograph of a growth front between several domains in melt-processed Y-Ba-Cu-O. Regions marked "A" show platelet terminations; regions marked "B" show the retained liquid phase penetrating the region between adjacent platelets. (b) SEM image of a fractured Y-Ba-Cu-O melt-processed domain showing terminations within the domain.

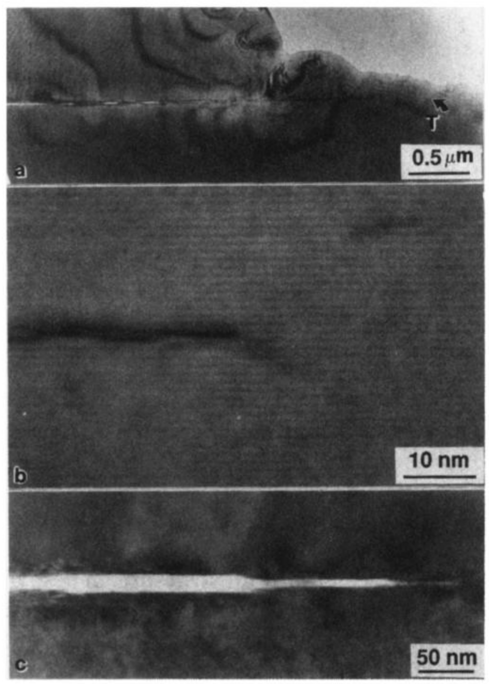

FIG. 7. (a) TEM image showing a gap terminating at the position marked "T." (b) Higher magnification image of the termination point showing that the material beyond the termination is continuous. (c) Region along the gap showing a stepwise narrowing of the gap.

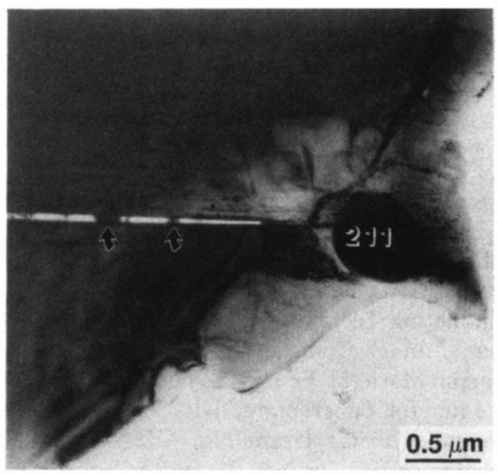

FIG. 8. Gap terminating near a 2:1:1 particle. The material to the right of the 2:1:1 particle is continuous. Diffraction contrast from crystalline material is seen within the gap region.